RESEARCH ARTICLE

Cationic Bis(Gold) Indenyl Complexes

Brady L. Slinger,[a] Jiaqi Zhu,[a] and Ross A. Widenhoefer*[a]

[a] *B. L. Slinger, J. Zhu, Prof. Dr. R. A. Widenhoefer*
Department of Chemistry
Duke University
French Family Science Center, Durham, NC, 27708-0346 (USA)
E-mail: rwidenho@chem.duke.edu

Supporting information for this article is given via a link at the end of the document.

Abstract: Reaction of (**P**)AuOTf [**P** = P(*t*-Bu)$_2$*o*-biphenyl] with indenyl- or 3-methylindenyl lithium led to isolation of gold η^1-indenyl complexes (**P**)Au(η^1-inden-1-yl) (**1a**) and (**P**)Au(η^1-3-methylinden-1-yl) (**1b**), respectively, in >65% yield. Whereas complex **1b** is static, complex **1a** undergoes facile, degenerate 1,3-migration of gold about the indenyl ligand ($\Delta G^{\ddagger}_{153K}$ = 9.1 ± 1.1 kcal/mol). Treatment of complexes **1a** and **1b** with (**P**)AuNTf$_2$ led to formation of the corresponding cationic bis(gold) indenyl complexes *trans*-[(**P**)Au]$_2$(η^1,η^1-inden-1,3-yl) (**2a**) and *trans*-[(**P**)Au]$_2$(η^1,η^2-3-methylinden-1-yl) (**2b**), respectively, which were characterized spectroscopically and modeled computationally. Despite the absence of aurophilic stabilization in complexes **2a** and **2b**, the binding affinity of mono(gold) complex **1a** toward exogenous (**P**)Au$^+$ exceed that of free indene by ~350-fold and similarly the binding affinity of **1b** toward exogenous (**P**)Au$^+$ exceed that of 3-methylindene by ~50-fold. The energy barrier for protodeauration of bis(gold) indenyl complex **2a** with HOAc was ≥8 kcal/mol higher than for protodeauration of mono(gold) complex **1a**.

Introduction

A number of mononuclear gold complexes bearing unsaturated σ-hydrocarbyl groups react with an exogenous 12-electron gold fragment (LAu$^+$) to form cationic bis(gold) complexes.[1] Included in this family of complexes are cationic bis(gold) vinyl,[2,3] aryl,[4] and heteroaryl[5] complexes which typically adopt a *gem*-diaurated structure stabilized by an aurophilic Au-Au interaction,[6] and bis(gold) alkynyl complexes that adopt a highly fluxional σ,π structure (Figure 1).[7,8] Importantly, these bis(gold) complexes often display markedly different reactivity vis-à-vis their mononuclear counterparts, most notably the significantly diminished reactivity toward electrophilic deauration.[2,3,7] For this reason, and due to the oftentimes highly favorable formation of bis(gold) complexes,[9] bis(gold) complexes are relevant to a range of gold(I)-catalyzed transformations, behaving either as active catalysts[10] or more often as off-cycle catalyst reservoirs.[3,8] As such, a meaningful understanding of gold(I) catalysis often requires consideration of the formation and consumption of bis(gold) intermediates.

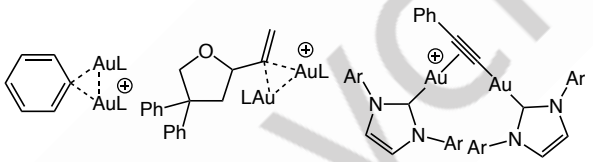

Figure 1. Representative examples of cationic bis(gold) aryl (left), vinyl (center), and alkynyl (right) complexes.

Gold η^1-allyl complexes have been invoked as reactive intermediates in a number of gold(I)-catalyzed transformations that are generated, for example, by the addition of nucleophiles to gold vinyl carbene complexes or to the sp carbon of gold π-allene complexes.[11] In contrast to the numerous examples of late transition metal η^3-allyl complexes,[12] well-defined gold allyl complexes are rare and biased toward η^1-coordination owing to the strong tendency of gold(I) to form linear 14-electron complexes.[13-17] Although no simple aliphatic allyl gold complex has been structurally characterized, spectroscopic and computational analyses of these complexes point to η^1-coordination of the allyl group.[16,18-21] Structurally characterized gold cyclopentadienyl complexes display an intermediate η^1/η^3 coordination mode with a shorter Au–C1 bond (2.15-2.20 Å) and longer Au–C2/C5 bonds (2.6-2.8 Å).[13,22] Owing to the nominal contribution of π-C=C bonding to the stabilization of gold allyl complexes, we considered that, by analogy to gold vinyl and alkynyl complexes, the allylic C=C bond of gold allyl complexes might bind to an exogenous 12-electron gold fragment to form cationic bis(gold)allyl complexes. Here we report that mononuclear gold η^1-inden-1-yl complexes react with exogenous LAu$^+$ to form cationic bis(gold) indenyl complexes in which the two gold fragments bind to opposite faces of the indenyl ligand in either an η^1,η^1 or η^1,η^2 orientation.

Results and Discussion

Mono(gold) Indenyl Complexes. For our investigation we sought gold η^1-allyl complexes that were (1) symmetrically and (2) differentially substituted at the allylic C1 and C3 positions that also contained a phosphine supporting ligand as a spectroscopic handle. Although simple aliphatic gold η^1-allyl complexes have been reported,[15,16] all our efforts to isolate such compounds were unsuccessful. For this reason, we targeted the gold η^1-indenyl complexes (**P**)Au(η^1-inden-1-yl) (**1a**) and (**P**)Au(η^1-3-

methylinden-1-yl) (**1b**) [**P** = P(*t*-Bu)$_2$*o*-biphenyl, i.e. JohnPhos], inspired by Hashmi's recent disclosure of 3-substituted gold(η^1-inden-1-yl) NHC complexes formed via the ring opening of gold cyclopropenyl complexes.[13] Because this approach appeared unsuitable for the formation of the parent gold indenyl complex **1a**, we instead explored a transmetallation approach analogous to those used to synthesize gold cyclopentadienyl and fluorenyl complexes.[22,23] To this end, reaction of (**P**)AuOTf with indenyl- or 3-methylindenyl lithium in THF at 25 °C for 12 h led to isolation of gold η^1-indenyl complexes **1a** and **1b**, respectively, in ≥66% yield (Scheme 1). Employing a slight deficiency of (**P**)AuOTf in these procedures proved critical to avoid contamination of **1a** and **2a** with the corresponding bis(gold) complexes (see below). Compounds **1a** and **1b** could be stored for several days at –4 °C in the solid state without significant decomposition but decomposed with a half-life of ~2.3 h in solution at room temperature.

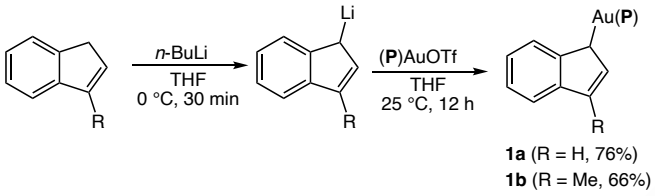

Scheme 1. Synthesis of gold η^1-indenyl complexes **1a** and **1b** via reaction of indenyl lithium reagents with (**P**)AuOTf.

Variable temperature NMR spectroscopy of **1a** established a gold η^1-indenyl complex that undergoes facile, degenerate 1,3-migration of gold about the indenyl ligand (Scheme 2). For example, the ^{1}H NMR spectrum of **1a** at –80 °C displayed a pair of broadened one-proton resonances at δ 3.03 and 6.41 ($\nu_{1/2}$ = 22 Hz) assigned to the indenyl C1 and C3 protons, respectively, a sharp one proton doublet at δ 6.63, assigned to the indenyl C2 proton, and unresolved multiplets at δ 6.9 and 7.4 assigned to the C4-C7 indenyl protons. Similarly, the ^{13}C NMR spectrum at –80 °C displayed broad resonances at δ 61 and 117 assigned to the indenyl C1 and C3 carbon atoms, respectively. As the temperature was raised, the indenyl C1 and C3 proton resonances broadened and coalesced ($T_c \approx$ –20 °C), forming a time-averaged two-proton doublet of doublets at δ 4.90 (J_{PH} = 7.8 Hz, J_{HH} = 3.3 Hz) at 25 °C (Figure 2). Over the same temperature range, the indenyl C4-C7 resonances broadened and coalesced to form an AA'XX' pattern at δ 7.38 and 6.95 at 25 °C. The room temperature ^{13}C NMR spectrum displayed a broad singlet at δ 89 assigned to the time-averaged C1 and C3 carbon atoms. Line shape analysis of the indenyl C1 and C3 ^{1}H NMR resonances over the temperature range –80 to 25 °C established the activation parameters for the isomerization of **1a** of $\Delta H^{\ddagger}$ = 12.9 ± 0.9 kcal/mol, $\Delta S^{\ddagger}$ = 15 ± 4 e.u., and $\Delta G^{\ddagger}_{253K}$ = 9.1 ± 1.3 kcal/mol (Figure 2).

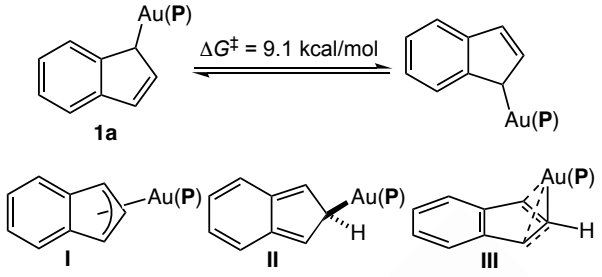

Scheme 2. Fluxional behavior and potential intermediates and/or transition states for the isomerization of **1a**.

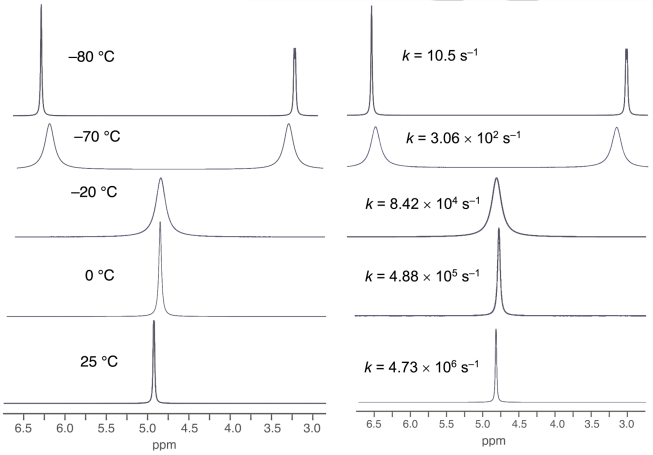

Figure 2. Temperature dependence of the indenyl C1 and C3 ^{1}H NMR resonances of **1a** from –80 to 25 °C in CD_2Cl_2 (left column) and simulated spectra (right column).

We initially considered two mechanisms for the enantiomerization of **1a** involving either (1) stepwise or concerted 1,3-migration of gold via the 16-electon η^3-allylic intermediate or transition state **I** or (2) consecutive [1,5]-sigmatropic rearrangements via the gold isoindenyl intermediate **II** (Scheme 2). The former has been documented for the isomerization many coordinatively unsaturated late transition metal allyl complexes while the latter has been postulated for the isomerization of a number of transition metal η^1-indenyl complexes[24-27] and gold(I) cyclopentadienyl complexes.[22] However, the previously computed activation barriers for the $\eta^1 \rightarrow \eta^3$ isomerization of gold secondary aliphatic η^1-allyl complexes range from $\Delta G^{\ddagger}$ = 18.1 to 26.3 kcal/mol,[19-21] which are significantly larger than the value determined experimentally for the isomerization of **1a** ($\Delta G^{\ddagger}$ = 9.1 kcal/mol). Similarly, although activation barriers as low as $\Delta G^{\ddagger}$ = 12 kcal/mol have been measured for the isomerization of a coordinatively saturated late transition metal η^1-indenyl complex,[25] [1,5]-sigmatropic rearrangements typically display negative activation entropies,[28] in contrast to the rather large positive activation entropy determined for the isomerization of **1a** ($\Delta S^{\ddagger}$ = 15 ± 4 eu).

To gain insight into the mechanism of the 1,3-migration of gold about the indenyl ligand of **1a**, we investigated this process computationally at the SMD(DCE)/TPSSh/ECP60MDF-aug-cc-pVTZ//B3LYP/ECP60MDF-6-31G(d) level of theory.

Trimethylphosphine was employed as the supporting ligand in place of P(*t*-Bu)$_2$*o*-biphenyl for computational simplicity and these structures are designated with an asterisk to distinguish from the parent complexes. The ground state structure calculated for **1a*** was in full accord with a gold η^1-indenyl species, consistent with our experimental observations regarding **1a**. In particular, the calculated Au–C1 bond distance (2.124 Å), the Au–C1–C2 (107.2°) and Au–C1–C9 (108.6°) bond angles, and the C1–C2 (1.489 Å) and C2–C3 (1.362 Å) bond lengths are typical of an Au-C(sp^3) bond (Figure 3). A PES scan of **1a*** as a function of the Au–C2–C1 bond angle located no additional local minima with **1a*-TS** representing the transition state for the enantiomerization of **1a*** with a free energy 7.4 kcal/mol greater than **1a*** at 298 K, which is not significantly different from the experimentally determined energy barrier ($\Delta G^{\ddagger}_{298K}$ = 8.4 ± 1.5 kcal/mol).

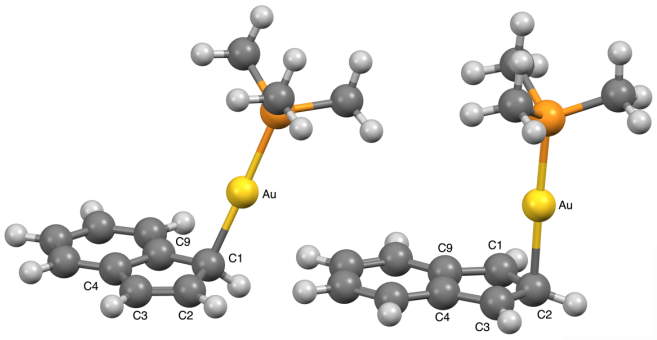

Figure 3. Ball and stick representations of the optimized ground state structures **1a*** and **1a*-TS**. Calculated bond lengths (Å) and bond angles (°) for **1a***: C1–C2 = 1.489, C2–C3 = 1.362, Au–C1 = 2.124, Au–C2 = 2.932, Au–C9 = 2.961, Au–C1–C2 = 107.2, Au–C1–C9 = 108.6. Au–C1–C2–C3 = 109.7, Au–C1–C9–C4 = 108.9. For **1a*-TS**: C1–C2 = 1.444, C2–C3 = 1.444, Au–C1 = 2.624, Au–C2 = 2.203, Au–C3 = 2.629, Au–C2–C1 = 89.7, Au–C2–C3 = 89.5. Au–C2–C1–C9 = 89.9, Au–C2–C3–C4 = 90.1.

The optimized structure of **1a*-TS** corresponds to neither a typical π-allyl structure nor a σ-isoindenyl structure. Rather, **1a*-TS** adopts an intermediate η^1/η^3 coordination mode that closely resembles the structures of gold cyclopentadienyl complexes (**III**, Scheme 2, Figure 3).[13,22] Transition state **1a*-TS** displays ~C2 symmetry with an Au–C2 bond (2.203 Å) that is ~0.8 Å longer than is the Au–C1 bond of **1a*** with weak (~2.62 Å) interactions between Au and the C1 and C3 carbon atoms (Figure 3). The Au(PMe$_3$) fragment is positioned perpendicular to the indenyl plane with Au–C2–C1 and Au–C2–C3 bond angles of ~90 ° and C1–C2 and C2–C3 bond lengths of 1.444 Å. The primary gold-indenyl bonding interaction in **1a*-TS** involves overlap of the occupied symmetric 3π_b indenyl orbital with the P–Au anti-bonding orbital.

In contrast to complex **1a**, variable-temperature analysis of the gold (3-methyl-inden-1-yl) complex **1b** revealed no fluxional behavior, consistent with Hashmi's observations.[13] The ^{1}H NMR spectrum of **1b** at -80 °C displayed a one proton doublet at δ 2.82 (J_{PH} = 14.7 Hz) and a one proton singlet at δ 6.25 assigned to the indenyl C1 and C2 protons, respectively. Warming the solution to 25 °C led to no detectable change in the ^{1}H NMR spectrum and gave rise to no signals that could be attributed to the isomeric gold (1-methyl-inden-1-yl)complex **2a'**, indicating that the indenyl 3-methyl group hinders the formal 1,3 migration pathway or, more likely, that **2a'** is significantly less stable than is **2a**, as has been validated computationally.[19-21]

Bis(gold) Indenyl Complexes. The gold η^1-indenyl complexes **1a** and **1b** reacted rapidly with exogenous (**P**)Au$^+$ to form cationic bis(gold) indenyl complexes. For example, when a ~1:1 mixture of **1a** (30 mM) and the gold bistriflimide complex (**P**)AuNTf$_2$ [NTf$_2$ = (CF$_3$SO$_2$)$_2$N] was dissolved in CD$_2$Cl$_2$ (0.60 mL) at room temperature, ^{31}P NMR analysis of the resulting solution at –80°C revealed complete consumption of **1a** to form the cationic bis(gold)indenyl complex {*trans*-[(**P**)Au]$_2$(η^1,η^1-inden-1,3-yl)}$^+$ NTf$_2^-$ (**2a**) which accounted for >95% of the reaction mixture (Scheme 3). Binding of exogenous (**P**)Au$^+$ to **1b** was less favorable than to **1a** and reaction of a ~1:1 mixture of **1b** and (**P**)AuNTf$_2$ led to formation of the bis(gold) indenyl complex {*trans*-[(**P**)Au]$_2$(η^1,η^2-3-methylinden-1-yl)}$^+$ NTf$_2^-$ (**2b**) in ~75% yield along with **1b** and (**P**)AuNTf$_2$, although formation of **2b** could be driven to completion with excess (**P**)AuNTf$_2$ (Scheme 3). Addition of pyridine (≥1 equiv) to solutions of either **2a** or **2b** led to quantitative regeneration of **1a** and **1b**, respectively (Scheme 3).

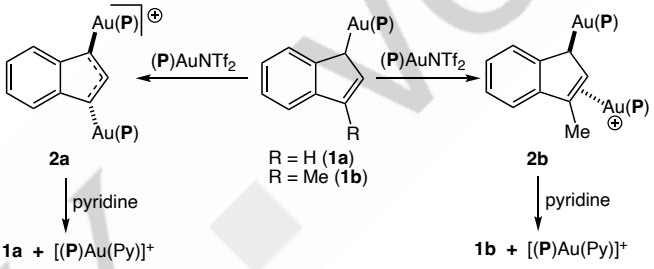

Scheme 3. Formation of bis(gold) indenyl complexes **2a** and **2b** (counterion = NTf$_2^-$).

Although stable indefinitely in solution at 25 °C, attempted isolation of **2a** or **2b** via precipitation from concentrated CH$_2$Cl$_2$ solutions led to decomposition and/or disproportionation. For this reason, complexes **2a** and **2b** were characterized in solution via multinuclear VTNMR spectroscopy. These data, in combination with computational analysis, are consistent with the formulation of **2a** as a static, *C*$_2$-symmetric complex formally comprising an indenyl anion with two *trans*-disposed (**P**)Au$^+$ fragments σ-bonded to the indenyl C1 and C3 atoms and **2b** as a static, unsymmetric complex with one (**P**)Au$^+$ fragment σ-bonded to the indenyl C1 atom and the second π-bonded to the indenyl C2=C3 bond (Scheme 3).

The ^{1}H NMR spectrum of **2a** at –80 °C displayed a phosphorous-coupled two-proton doublet at δ 4.20 (J_{PH} = 8.0 Hz) assigned to the chemically equivalent indenyl C1 and C3 protons, a one proton singlet at δ 6.97 assigned to the indenyl C2 proton, neither of which displayed any detectable excess broadening, and a pair of phosphorous-coupled doublets at δ 1.09 (J = 15.8 Hz) and δ 0.77 (J = 15.8 Hz) assigned to the diastereotopic phosphorous-bound *tert*-butyl groups. Similarly, the ^{13}C NMR spectrum of **2a** at –80 °C displayed a sharp phosphorous-coupled doublet at δ 79.9 (J_{CP} = 29 Hz) assigned to the chemically equivalent indenyl C1 and C3 carbon atoms and a singlet at δ 132 assigned to the indenyl C2 carbon atom. The ^{31}P NMR spectrum of **2a** at –80 °C displayed a sharp singlet at δ 60.6.

In comparison to **2a**, the ^{1}H NMR spectrum of **2b** at –80 °C displayed a one proton doublet at δ 3.16 (J_{PH} = 11.3 Hz) and a one proton singlet at δ 5.64 assigned to the C1 and C2 protons, respectively. The C2 proton resonance is shifted upfield relative to mono(gold) indenyl complex **1b** (Δδ = –0.61), as is typically

observed for gold π-alkene complexes,[29,30] while the C1 proton resonance is shifted downfield relative to **1b** (Δδ = +0.33), consistent with the depletion of electron density from the adjacent C=C bond owing to gold complexation. The ^{13}C NMR spectrum of **2b** at –80°C showed a sharp doublet at δ 66.7 (J_{CP} = 47 Hz) assigned to the indenyl C1 carbon atom and a singlet at δ 119.2 assigned to indenyl C2 carbon atom. The ^{31}P NMR spectrum of **2b** displayed a 1:1 ratio of resonances at δ 60.4 and 59.7, which established the presence of two chemically inequivalent (**P**)Au groups. The NMR spectra of **2a** remained invariant from –80 to 25 °C, arguing against any fluxional behavior.

Although the spectroscopy of complexes **2a** and **2b** is fully consistent with the proposed *trans*-η^1,η^1 and *trans*-η^1,η^2 structures, respectively, it is not sufficient to fully assign the structures of these complexes. For example, for both **2a** and **2b**, spectroscopy does not distinguish between a cis or trans arrangement of the two gold atoms and, in the case of **2a**, spectroscopy does not distinguish between a symmetric η^1,η^1-structure and a rapidly equilibrating η^1,η^2-complex, although the absence of detectable broadening in the –80 °C ^{1}H and ^{13}C NMR spectra of **2a** would require such a fluxional process to be exceedingly facile. To address these structural ambiguities, we investigated the relative stabilities of the potential *cis*- and *trans*-η^1,η^1 and η^1,η^2 isomers of bis(gold) indenyl and 3-methylindenyl complexes computationally at the same level of theory and same ligand substitution employed for structures **1a*** and **1a*-TS** (Figure 4).

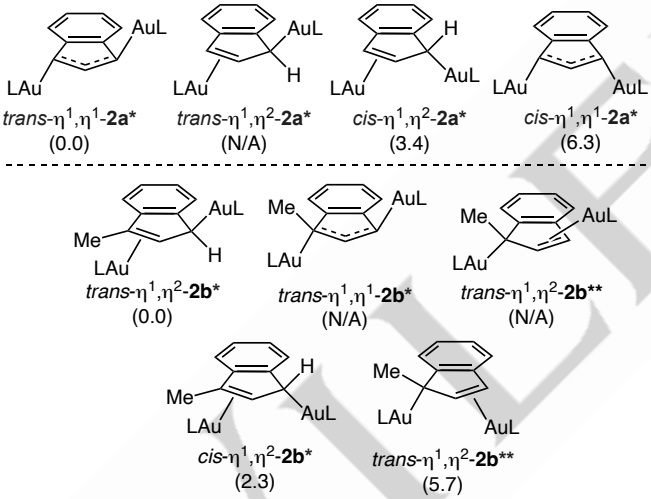

Figure 4. Optimized structures of the potential isomers of **2a*** (top) and **2b*** (bottom) with relative free energies in kcal/mol, where L = PMe_3. Structures indicated as N/A were not located as local minima on the potential energy surface.

For complex **2a***, *trans*-η^1,η^1-**2a*** and *cis*-η^1,η^2-**2a*** represent local minima with the former 3.4 kcal/mol more stable than the latter. A potential energy surface (PES) scan of *trans*-**2a*** geometries as a function of the Au2–C3–C4–C5 dihedral angle from 85.3° to 125.3° identified no additional local minima (Figure 4). Similarly, a PES scan of *cis*-**2a*** geometries as a function of the Au1–Au2 distance located no additional local minima with *cis*-η^1,η^1-**2a*** representing the transition state for interconversion of the two *cis*-η^1,η^2-**2a*** enantiomers residing 2.9 kcal/mol above *cis*-η^1,η^2-**2a***.

The ground-state structure *trans*-η^1,η^1-**2a*** is C_2 symmetric with the gold atoms positioned nominally perpendicular to the indenyl plane but biased slightly toward C2 and bent away from the indenyl core with an Au1–C2 distance of 2.697 Å and Au1–C1–C2 bond angle of 93.3° as compared to an Au1–C9 distance of 2.931 Å and an Au–C1–C9 bond angle of 103.83° (Figure 5). In addition to the highly compressed Au1–C1–C2 and Au2–C3–C2 bond angles, the Au–C1/Au2–C3 bond distances in *trans*-η^1,η^1-**2a*** are 2.204 Å, which are ~0.1 Å longer than the Au–C bond of the related mono(gold) fluorenyl complex $(PPh_3)Au(\eta^1$-fluoren-9-yl) and the calculated Au–C bond of **1a***.[23] Similarly, the Wiberg bond indices[31] of these bonds (0.827) are lower than those of a typical Au–C σ-bond.[32] The Au–indenyl bonding in *trans*-η^1,η^1-**2a*** is interpreted through the orbital interactions of indenyl anion with a pair of $(PMe_3)Au^+$ groups (Figure 6). The primary gold-indenyl bonding interaction comprises overlap between the filled antisymmetric $2\pi_a$ and $1\pi_a$ indenyl orbitals with the symmetric combination of the P–Au anti-bonding orbitals [$\phi_a(\sigma^*)$] without any significant Au → indenyl backbonding interactions (Figure 6a).

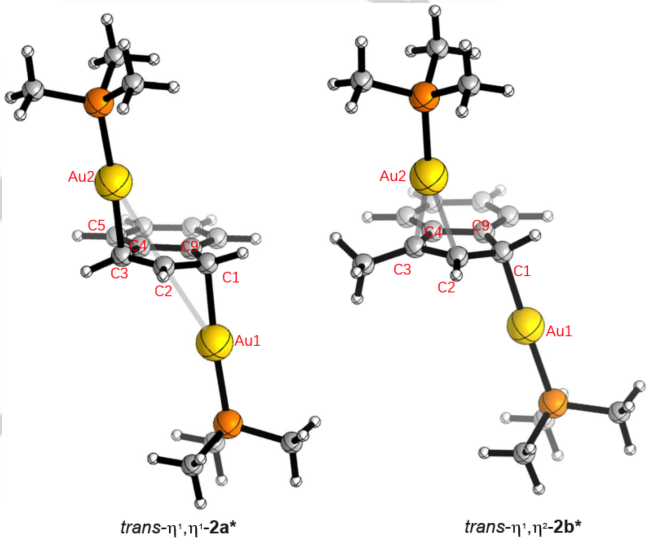

Figure 5. Ball and stick representation of the optimized ground state structures *trans*-η^1,η^1-**2a*** and *trans*-η^1,η^2-**2b***. Calculated bond lengths (Å) and bond angles (°) for *trans*-η^1,η^2-**2a***: C1–C2 = 1.432, Au1–C1 = 2.204, Au1–C2 = 2.697, Au–C1–C2 = 93.3, Au–C1–C9 = 103.8. Au–C1–C2–C3 = 103.95, Au–C1–C9–C4 = 93.62. For *trans*-η^1,η^2-**2b***: C1–C2 = 1.476, C2–C3 = 1.414, Au1–C1 = 2.16, Au2–C2 = 2.37, Au2–C3 = 2.33, Au–C1-C9 = 107.12, Au–C1-C9 = 104.94, Au2–C3–C2 = Au2–C2–C3 = 71.04, Au2–C3–C2 = 73.98 Au2–C3–C4 = 101.78.

For complex **2b***, *trans*-η^1,η^2-**2b***, *cis*-η^1,η^2-**2b***, and *cis*-η^1,η^2-**2b****, the latter containing a gold-methine σ-bond, represent local minima with *trans*-η^1,η^2-**2b*** residing 2.3 and 5.7 kcal/mol below *cis*-η^1,η^2-**2b*** and *cis*-η^1,η^2-**2b****, respectively (Figures 4 and 5). A PES scan of *trans*-**2b*** as a function of the Au2–C3–C4–C6 dihedral angle from 77.1 to 113.1° identified no additional local minima (Figure 4). In comparison to the Au–C bonds of *trans*-η^1,η^1-**2a***, the Au1–C1 bond of *trans*-η^1,η^2-**2b*** is slightly shorter (2.16 Å) with a Wiberg bond index of 0.939 and a Au1–C1–C2 bond angle of 104.9° that approaches that of idealized Au–C(sp^3) σ bond (Figure 5). The Au2–C3 (2.33 Å) and Au2–C2 (2.37 Å) bond distances, the Au2–C3–C2 (74.0°) and Au2–C2–C3 (71.0°) bond angles, and the Wiberg bond indices for Au2–C3 (0.596),

Au2–C2 (0.597) are consistent with a typical gold η^2-alkene bond.[29,30]

The Au–C σ-bond of **2b*** arises from overlap between the filled antisymmetric $2\pi_a$ and $1\pi_a$ indenyl orbitals with the P–Au anti-bonding orbital of one of the two Au(PMe_3) groups (Figure 6b). In comparison, the Au–C π-bond of **2b*** results from overlap of the both the filled antisymmetric $2\pi_a$ and $1\pi_a$ indenyl orbitals and the symmetric $3\pi_b$ indenyl orbital with the P–Au anti-bonding orbital of the second Au(PMe_3) group. As was the case with **2a***, no significant Au → indenyl backbonding interactions stabilize the Au–C π-bond.

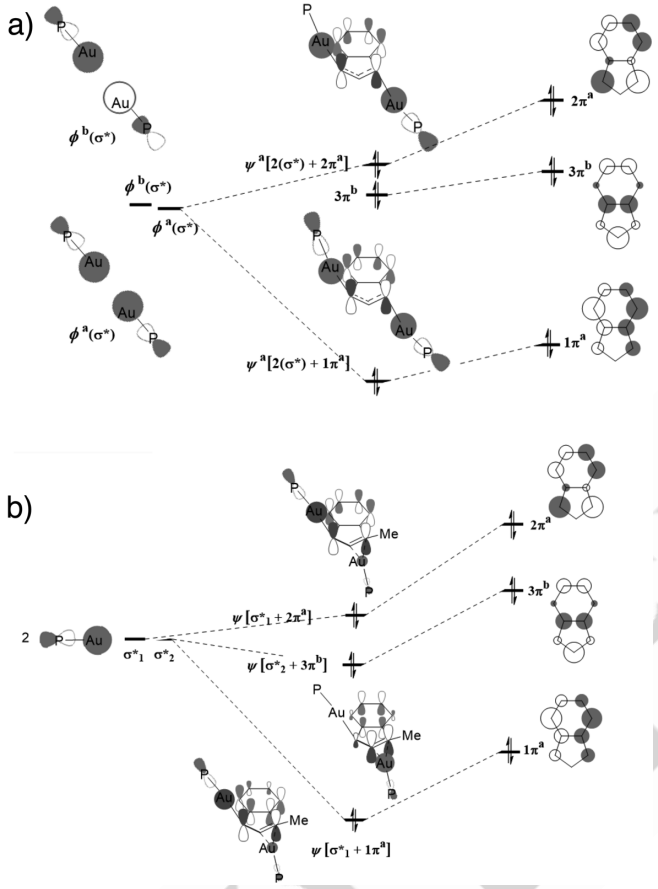

Figure 6. Orbital mixing diagrams describing the gold-indenyl bonding of (a) **2a*** and (b) **2b***.

Whereas dinuclear η^1,η^2-allyl complexes analogous to **2b** are known for Fe,[33] Pt[34], and mixed metal systems,[35,36] the *trans*-η^1,η^1 structure of **2a** appears unique among transition metal complexes. The closest analogs to **2a** are the dinuclear palladium(I) and nickel(I) μ-allyl, μ-cyclopentadienyl and μ-indenyl complexes, but here too, the structure and bonding of these complexes are distinct from **2a**.[37-40] Firstly, these M_2(μ-allyl) complexes contain an M–M bond and an additional bridging ligand that enforces a cis-arrangement of metals about the bridging allyl ligand. Secondly, bonding of the allyl group to the dimetallic core in these complexes is realized through a combination of π-donation and π-backbonding interactions, the former involving overlap of the antisymmetric π-allyl HOMO with the M–M dσ antibonding orbital and the latter involving overlap of the M–M dσ bonding orbital with the symmetric π-allyl LUMO.[40] The contribution of the backbonding interaction to the M_2-π-allyl bond is manifested in a much shorter bond between the metal atom and the internal allylic carbon atom (C_{int}) than is calculated for **2a***, for which M → allyl backbonding is largely absent. In particular, the M–C_{int} bond of dinuclear Pd(I) and Ni(I) μ-allyl complexes is 0.2 - 0.3 Å longer than are the M–$C_{terminal}$ bonds as compared to the ~0.5 Å difference in the Au–C2 and Au–C1/C3 bonds of **2a***. The absence of significant π-backbonding in complex **2a*** is reminiscent of the poor backbonding in gold π-alkene complexes.[29,30]

We sought to quantify the relative binding affinities of the mononuclear gold (η^1-inden-1-yl) complexes **1a** and **1b** and their unmetallated counterparts indene and 3-methylindene, respectively, toward exogenous (**P**)Au^+. To this end, we determined equilibrium constants for the displacement of the weakly coordinating ligand $NCAr_F$ [Ar_F = 3,5-$C_6H_3(CF_3)$] from [(**P**)Au($NCAr_F$)]$^+$ SbF_6^- (**3**) with **1a**, **1b**, indene, and 3-methylindene in CD_2Cl_2 at –80 °C employing ^{31}P NMR analysis (Scheme 4).[29] The equilibrium constant for displacement of $NCAr_F$ from **3** by **1a** of K_{eq} = [**1a**][**3**]/[**2a**][$NCAr_F$] = 75 ± 4 was ~3.5 fold larger than was the equilibrium constant for displacement of $NCAr_F$ from **3** by **1b** (K_{eq} = 20 ± 1) and ~350 times larger than the equilibrium constant for displacement of $NCAr_F$ from **3** by indene (K_{eq} = 0.21 ± 0.01). In comparison, binding affinity of gold 3-methylindenyl complex **1b** toward exogenous (**P**)Au^+ exceeds that of free 3-methylindene by a factor of ~50 (Scheme 4).

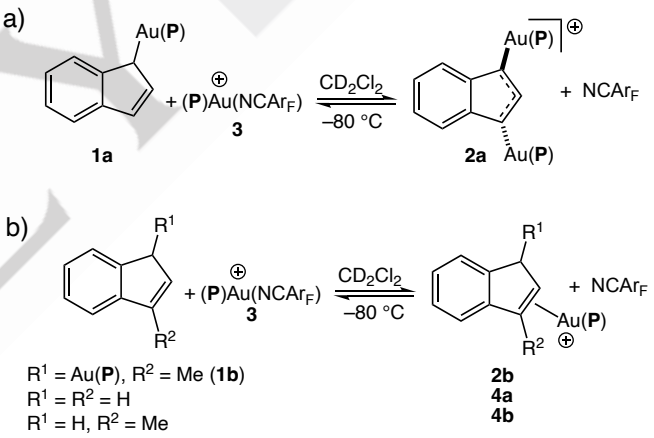

Scheme 4. a) Reaction of **1a** with **3** (counterion = SbF_6^-). b) Reaction of **1b**, indene, and 3-methylindene with **3** (counterion = SbF_6^-).

The enhanced binding affinity of mono(gold) indenyl complexes **1a** and **1b** toward exogenous gold relative indene and 3-methyl indene, respectively, without any direct aurophilic interaction is reminiscent of the enhanced binding affinity of gold σ-alkynyl complexes toward exogenous (L)Au^+ relative to the corresponding terminal alkynes.[7] In both cases, the enhanced binding affinity of the gold σ-complex toward LAu^+ relative to the unmetallated hydrocarbon is presumably due to the greater σ-donor ability of LAu relative to H,[41] which increases the electron donor ability of the gold σ-complex relative to the unmetallated hydrocarbon. The greater affinity of **1a** toward exogenous (**P**)Au^+ vis-a-vis **1b** might be due simply to the greater stability of the **1b** relative to **1a**.

A notable characteristic of bis(gold) vinyl, aryl, and alkynyl complexes is the markedly diminished reactivity of these complexes toward electrophilic deauration relative to the

corresponding mono(gold) complex.[1-7] We therefore sought to similarly gauge the reactivity of monogold and bis(gold) indenyl complexes toward protodeauration. To this end, treatment of **1a** (42 mM) with excess HOAc (0.42 M) in CD_2Cl_2 at –80 °C led to rapid (≤ 45s), quantitative protodeauration of **1a** to form a ~1:1 mixture of indene and the bis(gold) complex **2a**, which was stable indefinitely (45 min) under these conditions (Scheme 5a). In a separate experiment, treatment of **2a** (42 mM) with HOAc (0.42 M) in CD_2Cl_2 at –20 °C for 2h led to no detectable protodeauration (Scheme 5b). From these data, we can estimate a lower limit for the difference in the activation free energy for protodeauration of **1a** and **2a** of $\Delta\Delta G^{\ddagger}$ = ≥8 kcal/mol.

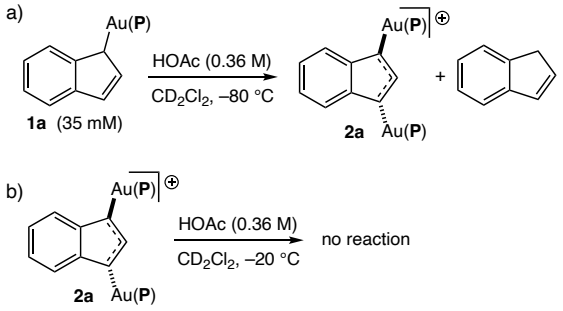

Scheme 5. (a) Protodeauration of **1a** with HOAc at –80 °C and (b) attempted protodeauration of **2a** with HOAc at –20 °C.

Conclusion

We have shown that mononuclear gold η^1-indenyl complexes react with exogenous (**P**)Au^+ to form cationic bis(gold)indenyl complexes that adopt either a *trans*-(η^1,η^1-inden-1,3-yl) structure in the case of **2a** or a *trans*-(η^1,η^2-3-methylinden-1-yl) structure in the case of **2b**. In contrast to the large body of work describing the synthesis and reactivity of bis(gold) vinyl, aryl, and alkynyl complexes, complexes **2a** and **2b** represent the first examples of cationic bis(gold) allyl complexes. Whereas dinuclear η^1,η^2-allyl complexes analogous to **2b** are known, the *trans*-η^1,η^1 structure of **2a** is unique. DFT analysis of complex **2a*** points to overlap of the antisymmetric $2\pi_a$ and $1\pi_a$ indenyl orbitals with the symmetric combination of the Au–P antibonding orbitals as the dominant gold-indenyl bonding interaction without significant back bonding interactions.

The Au-indenyl binding of **2a*** is distinct from that of dinuclear palladium and nickel μ-allyl, μ-cyclopentadienyl and μ-indenyl complexes owing to the presence of strong backbonding interactions in these latter complexes. Worth noting is that computational analyses of these M_2(μ-allyl), M_2(μ-indenyl), and M_2(μ-cyclopentadienyl) complexes point to analogous bonding interactions in all cases, suggesting the *trans*-η^1,η^1 structure of **2a** might also be general to cationic bis(gold) allyl complexes. At the same time, slight perturbation of the indene structure arising from substitution of C3–H for C3-methyl biases the structure toward a *trans*-η^1,η^2-bonding arrangement as observed for **2b**. Aside from these two data points, the factors that control the binding mode of cationic bis(gold) allyl complexes remains undefined and will be the subject of continued investigation in our laboratory.

The mono(gold) indenyl complexes **1a** and **1b** display much higher binding affinity toward exogenous (**P**)Au^+ than do their unmetallated counterparts, **1a** in particular, presumably due to the greater σ-donor ability of the (**P**)Au fragment relative to a hydrogen atom. Furthermore, the reactivity of the bis(gold) indenyl complex **2a** toward protodeauration was orders of magnitude slower than was protodeauration of mono(gold) indenyl complex **1a**, which mirrors the behavior of cationic bis(gold) vinyl, aryl, and alkynyl complexes. Taken together, these observations suggest that bis(gold)allyl complexes might be kinetically relevant intermediates in gold(I)-catalyzed processes that involve gold η^1-allyl intermediates, but here too, further investigation is required to evaluate this possibility.

Experimental Section

[P(*t*-Bu)$_2$*o*-biphenyl]Au(η^1-inden-1-yl) (1a). A solution of indene (50 μL, 0.43 mmol) in THF (0.5 mL) was added via syringe to a solution of *n*-butyllithium (0.16 mL, 0.39 mmol, 2.5 M in hexanes) in THF (6 mL) at 0°C and the solution was stirred for 1 h. A solution of (**P**)AuOTf (0.25 g, 0.39 mmol) in THF (4 mL) was added via syringe to the solution of indenyl lithium at 0 °C and the resulting solution was stirred overnight at room temperature. The solvent was evaporated to dryness under vacuum and the residue was washed with hexane (3 × 8 mL) to give a brown solid that was dissolved in CH_2Cl_2, filtered (0.22 μM mesh) and evaporated under vacuum to give **1a** (0.18 g, 76%) as a pale brown solid. ^{1}H NMR ($CDCl_3$, 400 MHz, 25 °C): δ 7.80 (td, *J* = 7.2, 1.2 Hz, 1 H), 7.61-7.37 (m, 5H), [7.40, 6.95 (AA'XX', $J_{AA'}$ = 6.6 Hz, $J_{XX'}$ = 0.9 Hz, J_{AX} = 7.6 Hz, $J_{AX'}$ = 1.2 Hz, 4H)], 7.29 - 7.22 (m, 3H), 6.97 (dd, *J* = 5.7, 3.1 Hz, 2H), 6.70 (t, *J* = 3.3 Hz, 1H), 4.90 (dd, *J* = 7.8, 3.3 Hz, 2H), 1.14 (d, *J* = 14.8 Hz, 18H). ^{1}H NMR (CD_2Cl_2, 700 MHz, -80 °C): δ 7.78-7.15 (m, 11H), 6.89 (s, 2H), 6.63 (s, 1H), 6.41 (br s, 1H), 3.03 (br d, 14.0 Hz, 1H), 1.09 (br d, *J* = 20.3 Hz, 18H). ^{13}C{^{1}H} NMR (CD_2Cl_2, 176 MHz, –80°C): δ 148.85 (d, *J* = 16.1 Hz), 144.13, 143.35, 143.14 (d, *J* = 6.1 Hz), 140.50, 137.84 (d, *J* = 5.2 Hz), 134.60, 134.25, 132.17 (d, *J* = 7.8 Hz), 131.23, 129.62, 129.27, 127.83, 127.16, 126.95, 126.52, 125.71, 124.03, 123.36, 121.37 (br), 120.47, 119.82 (br), 119.21 (br), 116.37 (br), 60.77 (d, *J* = 68.1 Hz), 36.06 (d, 20.8 Hz), 29.83. ^{31}P{^{1}H} NMR (CD_2Cl_2, 283 MHz, –80°C): δ 62.6. ^{31}P{^{1}H} NMR ($CDCl_3$, 162 MHz, 25°C): δ 64.14. HRMS (APCI/APPI) calcd (found) for $C_{29}H_{34}AuP$: 610.2100 (610.2062).

[P(*t*-Bu)$_2$*o*-biphenyl]Au(η^1-3-methylinden-1-yl) (1b). Reaction of (**P**)AuOTf with 3-methylindenyl lithium employing a procedure analogous to that used to synthesize **1a** gave **1b** in 66% yield as a pale brown solid. ^{1}H NMR (CD_2Cl_2, 700 MHz, -80 °C): δ 7.82-6.9 (m, 13H), 6.25 (s, 1H), 2.82 (d, *J* = 14.7 Hz, 1H), 2.19 (s, 3H), 1.16 (m, 18H). ^{13}C{^{1}H} NMR (CD_2Cl_2, 176 MHz, –80°C): δ 150.69 (d, *J* = 3.5 Hz), 148.75 (d, *J* = 16.2 Hz), 143.02 (d, *J* = 5.7 Hz), 141.67, 135.05 (d, *J* = 5.1 Hz), 134.33, 132.09 (d, *J* = 7.7 Hz), 129.45, 129.27, 128.93, 127.78, 127.47 (d, *J* = 4.7 Hz), 127.26, 126.86, 126.35 (d, *J* = 4.8 Hz), 125.85 (d, *J* = 3.8 Hz), 121.55, 119.91, 119.40, 116.97, 58.27 (d, *J* = 63.8 Hz), 36.09 (dd, *J* = 20.1, 12.3 Hz), 29.83 (d, *J* = 57.0 Hz), 12.57. ^{31}P{^{1}H} NMR (CD_2Cl_2, 283 MHz, -80°C): δ 63.3. HRMS (APCI/APPI) calcd (found) for $C_{30}H_{36}AuP$: 624.2200 (624.2218).

{[P(*t*-Bu)$_2$*o*-biphenyl]$_2$Au(η^1,η^1-inden-1,3-yl)}$^+$ NTf_2^- (2a). A solution of **1a** (15 mg, 0.03 mmol) and (**P**)$AuNTf_2$ (19 mg, 0.03 mmol) in CD_2Cl_2 (600 μL) was added to NMR tube, shaken, and cooled to –80°C. ^{31}P NMR analysis of the solution revealed formation of **2a** which constituted >95% of the reaction mixture. ^{1}H NMR (CD_2Cl_2, 700 MHz, -80 °C): δ 7.81-7.13 (m, 22H), 7.04 (s, 2H), 6.97 (s, 1H), 4.20 (d, *J* = 8.0 Hz, 2H), 1.08 (d, *J* = 15.8 Hz, 18H), 0.76 (d, *J* = 15.8 Hz, 18H). ^{13}C{^{1}H} NMR (CD_2Cl_2, 176 MHz, –80 °C): δ 148.03 (d, *J* = 14.6 Hz), 142.76 (d, *J* = 6.6 Hz), 141.67 (d, *J* = 1.6 Hz), 133.28, 132.12 (d, *J* = 7.3 Hz), 131.34, 130.17, 129.49, 129.25, 128.41, 127.98, 126.91, 126.67, 124.49, 124.24, 121.91, 120.73, 118.9 (q, J_{CF} = 320 Hz), 79.21 (d, *J* = 29 Hz), 36.11 (d, *J* = 23 Hz), 35.88 (d, *J* = 24 Hz), 29.64 (br), 29.00 (br). ^{31}P{^{1}H} NMR (CD_2Cl_2, 283 MHz, -80°C): δ 61.0.

{[P(*t*-Bu)$_2$*o*-biphenyl]$_2$Au(η^1,η^2-3-methylinden-1-yl)}$^+$ NTf$_2^-$ (2b). A solution of gold indenyl complex **2a** (15 mg, 0.03 mmol) and (**P**)AuNTf$_2$ (13 mg, 0.03 mmol) in CD_2Cl_2 (600 µL) were added to NMR tube, shaken, and cooled to –80°C. ^{31}P NMR analysis of the solution revealed predominant (≥75%) formation of **2b** along with **1b** and (**P**)AuNTf$_2$. ^{1}H NMR (CD_2Cl_2, 700 MHz, -80 °C): δ 7.82-7.02 (m), 5.64 (s, 1H), 3.16 (d, *J* = 11.3 Hz, 1 H), 2.18 (s, 3H), 1.10 (d, *J* = 15.7 Hz, 18 H), 1.01 (d, *J* = 15.9 Hz, 18 H), 0.89 (d, *J* = 15.3 Hz, 18 H). ^{13}C{^{1}H} NMR (CD_2Cl_2, 176 MHz, -80°C): δ 148.2 (d, *J* = 15 Hz), 148.0 (d, *J* = 14 Hz), 143.0 (d, *J* = 4.5 Hz), 142.2 (d, *J* = 4.4 Hz), 139.7, 133.7, 133.1, 132.3 (d, *J* = 7.2 Hz), 132.0, 130.4, 130.0, 129.5 (d, *J* = 11 Hz), 129.3, 128.3, 128.2, 128.0, 127.6, 127.2, 126.4, 125.5, 125.3, 123.8, 123.0, 122.8, 121.5, 121.0, 120.9,119.2, 119.0 (q, J_{CF} = 321 Hz), 111.9 (d, *J* = 13 Hz), 66.7 (d, *J* = 47 Hz), 36.1 (m), 29.4 (br d, *J* = 76 Hz), 14.8. ^{31}P{^{1}H} NMR (CD_2Cl_2, 283 MHz, -80°C): δ 60.38, 59.73.

Equilibrium binding affinity of indene and 3-methylindene to (P)Au$^+$. A solution of indene (1.8 µL, 0.020 mmol) and [(**P**)Au(NCAr$_F$)]$^+$ SbF$_6^-$ [**3**; 15 mg, 0.020 mmol] in CD_2Cl_2 (600 µL) was added to an NMR tube, mixed thoroughly, and placed in the probe of an NMR spectrometer precooled at –80°C. ^{31}P NMR analysis of the solution revealed a 1.0:2.2 mixture of [(**P**)Au(η^2-indene)]$^+$ SbF$_6^-$ (**4a**) and **3**, which was characterized in solution by ^{1}H and ^{31}P NMR spectroscopy and by analogy to known cationic [(**P**)Au(η^2-styrenyl)]$^+$ SbF$_6^-$ complexes.[29] An equilibrium constant for the conversion of **3** to **4a** of K_{eq} = [**4a**][NCAr$_F$]/[indene][**3**] = 0.21 ± 0.01 was determined assuming [indene] = [**3**] and [NCAr$_F$] = [**4a**]. An equilibrium constant of K_{eq} = [**4b**][NCAr$_F$]/[3-methylindene][**3**] = 0.40 ± 0.02 was determined for the reaction of 3-methylindene with **3** employing a similar procedure and assumptions.

For 4a: ^{1}H NMR (CD_2Cl_2, 700 MHz, -80 °C): δ 8.42-7.04 (m), 6.77 (s, 1H), 5.81 (s, 1H), 3.55 (d, *J* = 24.0 Hz, 1H), 3.44 (d, *J* = 24.0 Hz, 1H) 1.00 (d, *J* = 16.5 Hz, 18H). ^{31}P{^{1}H} NMR (CD_2Cl_2, 283 MHz, -80°C): δ 63.9.

For 4b: ^{1}H NMR (CD_2Cl_2, 700 MHz, -80 °C): δ 8.42-7.04 (m), 4.76 (s, 1H), 3.28 (d, *J* = 23.4, Hz, 1H), 3.21, (d, *J* = 23.4 Hz, 1H), 2.46 (s, 3H), 1.23 (d, *J* = 16.5 Hz, 18H). ^{31}P{^{1}H} NMR (CD_2Cl_2, 283 MHz, -80°C): δ 63.9.

Equilibrium binding affinity of 1a and 1b to (P)Au$^+$. A solution of **1a** (15 mg, 0.03 mmol) and [(**P**)Au(NCAr$_F$)]$^+$ SbF$_6^-$ (**3**; 16 mg, 0.02 mol) in CD_2Cl_2 (600 µL) was added to an NMR tube, mixed thoroughly, and placed in the probe of an NMR spectrometer precooled at –80°C. ^{31}P NMR analysis of the solution revealed a 10.5:1.0:1.5 mixture of **2a**:**3**:**1a**. An equilibrium constant for the conversion of **1a** and **3** to **2a** and NCAr$_F$ of K_{eq} = [**2a**][NCAr$_F$]/[**1a**][**3**] = 75 ± 4 was determined assuming [NCAr$_F$] = [**2a**]. Similarly, rection of **1b** (15 mg, 0.02 mmol) and **3** (9.3 mg, 0.01 mmol) in CD_2Cl_2 (600 µL) at –80 °C formed a 6.5:1.0:2.1 mixture of **2b**:**3**:**1b**, which corresponds to an equilibrium constant for the conversion of **1b** and **3** to **2b** and NCAr$_F$ of K_{eq} = [**2b**][NCAr$_F$]/[**1b**][**3**] = 20 ± 1 assuming [NCAr$_F$] = [**2b**].

Protodeauration of 1a. Acetic acid (14.3 µL, 0.250 mmol) was added to an NMR tube containing a solution of **1a** (15 mg, 0.030 mmol) and CH_2Br_2 (2 mg, 0.012 mmol, internal standard) in CD_2Cl_2 (600 µL) at –80°C. The contents of the tube were mixed thoroughly and placed in the probe of an NMR spectrometer precooled at –80°C. A ^{31}P NMR spectrum recorded within ~45 s revealed ≥ 90% consumption of **1a** and formation of **2b** and a ^{1}H NMR spectrum recorded immediately thereafter revealed formation of **2b** in 45% yield (50% theoretical) and indene in 55%. Assuming ≥10% of unreacted **1a** would have been observed in the initial ^{31}P NMR spectrum, we can set a lower limit for the observed rate constant for protodeauration of $k_{obs} \geq 0.05$ s^{-1} ($t_{1/2} \leq 15$ s), which corresponds to an apparent activation free energy of $\Delta G^{\ddagger}_{193K}$ = 12.3 kcal/mol.

Protodeauration of 2a. Acetic acid (14.3 µL, 0.250 mmol) was added to a solution of **2a** (~0.030 mmol) and CH_2Br_2 (2 mg, 0.012 mmol, internal standard) in CD_2Cl_2 (600 µL) at -80°C. The contents of the tube were mixed thoroughly and placed in the probe of an NMR spectrometer precooled at –80°C. After 45 min at –80°C and 2 h at –20 °C, ^{31}P and ^{1}H NMR analysis of the solution revealed no detectable consumption of **2a**. Assuming 10% consumption of **2a** would have been observed in the ^{31}P NMR spectrum, we can set an upper limit for the observed rate constant for protodeauration of $k_{obs} \leq 1.2 \times 10^{-5}$ s^{-1} ($t_{1/2} \geq$ 16h), which corresponds to an apparent activation free energy of $\Delta G^{\ddagger}_{253K} \geq$ 20.4 kcal/mol.

Computational methods. All DFT calculations were performed by employing the Gaussian 16 program.[42] The B3LYP method[43] were used to locate all relevant minima and saddle points. The 6-31G(d) basis set[44] was applied for all the nonmetallic atoms and ECP60MDF pseudopotential with the corresponding ECP60MDF basis set[45] was applied for gold. All the stationary points were optimized in the gas-phase and frequency calculations were performed at the same level to evaluate the thermal corrections at 298 K without scaling. Single point energies based on the geometry structures obtained at the B3LYP level were calculated with TPSSh method[46] using aug-cc-pVTZ basis set[47] for nonmetallic atoms and Stuttgart pseudopotentials ECP60MDF with aug-cc-pVTZ-PP for gold. Solvation energies in CH_2Cl_2 were computed with the SMD[48] continuum model.

Acknowledgements

This work was supported by the NSF (CHE-2102653).

Keywords: Allyl Ligands • Gold • Density functional calculations, Isomerization • NMR spectroscopy

[1] D. Weber, M. R. Gagné, *Top. Curr. Chem.* **2014**, *357*, 167−212.

[2] a) G. Seidel, C. W. Lehmann, A. Fürstner, *Angew. Chem.* **2010**, *122*, 8644 – 8648; *Angew. Chem. Int. Ed.* **2010**, *49*, 8466 – 8470; b) A. Zhdanko, M. E. Maier, *Chem. Eur. J.* **2013**, *19*, 3932–3942; c) D. Weber, M. R. Gagné, *Chem. Sci.* **2013**, **4**, 335–338.

[3] a) T. J. Brown, D. Weber, M. R. Gagné, R. A. Widenhoefer, *J. Am. Chem. Soc.* **2012**, *134*, 9134–9137; b) D. Weber, M. A. Tarselli, M. R. Gagné, *Angew. Chem.* **2009**, *121*, 5843- 5846; *Angew. Chem. Int. Ed.* **2009**, *48*, 5733-5736; c) Y. Tang, J. Li, Y. Zhu, Y. Li, B. Yu, *J. Am. Chem. Soc.* **2013**, *135*, 18396-18405; d) A. Zhdanko, M. E. Maier, *Chem. Eur. J.* **2014**, *20*, 1918-1930.

[4] a) A. N. Nesmeyanov, E. G. Perevalova, K. I. Grandberg, D. A. Lemovskii, T. V. Baukova, O. B. Afanassova, *J. Organomet. Chem.* **1974**, *65*, 131-144; b) D. Weber, T. D. Jones, L. L. Adduci, M. R. Gagne, *Angew. Chem. Int. Ed.* **2012**, *51*, 2452 –2456; c) A. N. Nesmeyanov, E. G. Perevalova, K. I. Grandberg, D. A. Lemenovskii, *Izv. Akad. Nauk SSSR Ser. Khim.* **1974**, *5*, 1124 – 1137; d) M. Osawa, M. Hoshino, D. Hashizume, *Dalton Trans.* **2008**, 2248 – 2252; e) R. Uson, A. Laguna, E. J. Fernandez, A. Media, P. G. Jones, *J. Organomet. Chem.* **1988**, *350*, 129 – 138; f) H. Schmidbaur, Y. Inoguchi, *Chem. Ber.* **1980**, *113*, 1646-1653; g) J. E. Heckler, M. Zeller, A. D. Hunter, T. G. Gray, *Angew. Chem.* **2012**, *124*, 6026 -6030; *Angew. Chem. Int. Ed.* **2012**, *51*, 5924 –5928.

[5] K. A. Porter, A. Schier, H. Schmidbaur, *Organometallics* **2003**, *22*, 4922 – 4927.

[6] a) H. Schmidbaur, A. Schier, *Chem. Soc. Rev.* **2012**, *41*, 370−412; b) H. Schmidbaur, A. Schier, *Chem. Soc. Rev.* **2008**, *37*, 1931 –1951; c) H. Schmidbaur, *Gold Bull.* **2000**, *33*, 1 – 10; d) H. Schmidbaur, *Chem. Soc. Rev.* **1995**, *24*, 391 – 400.

[7] a) T. J. Brown, R. A. Widenhoefer, *Organometallics* **2011**, *30*, 6003 – 6009; b) A. Grirrane, H. Garcia, A. Corma, E. Ivarez, *ACS Catal.* **2011**, *1*, 1647 – 1653.

[8] a) A. Simonneau, F. Jaroschik, D. Lesage, M. Karanik, R. Guillot, M. Malacria, J.C. Tabet, J.P. Goddard, L. Fensterbank, V. Gandon, Y. Gimbert, *Chem. Sci.* **2011**, *2*, 2417 – 2422; b) C. Obradors, A.M. Echavarren, *Chem. Eur. J.* **2013**, *19*, 3547-355; c) A. Homs, C. Obradors, D. Leboeuf, A.M. Echavarren, *Adv. Synth. Catal.* **2014,** *356*, 221-228; d) A. Grirrane, H. Garcia, A. Corma, E. Alvarez, *Chem. Eur. J.* **2013**, *19*, 12239-12244.

[9] A. Zhdanko, M. E. Maier, *Organometallics* **2013**, *32*, 2000−2006.

[10] a) P. H. Y. Cheong, P. Morganelli, M. R. Luzung, K. N. Houk, F. D. Toste, *J. Am. Chem. Soc.* **2008**, *130*, 4517-4526; b) A. S. K. Hashmi, *Acc. Chem. Res.* **2014**, *47*, 864−876; c) X. Zhao, M. Rudolph, A. S. K. Hashmi, *Chem. Commun.* **2019**, *55*, 12127−12135; d) Y. Odabachian, X. F. Le Goff, F. Gagosz, *Chem. Eur. J.* **2009**, *15*, 8966-8970.

[11] a) R. R. Singh, R. S. Liu, *Adv. Synth. Catal.* **2016**, *358*, 1421-1427; b) M. Uemura, I. D. G. Watson, M. Katsukawa, F. D. Toste, *J. Am. Chem. Soc.* **2009**, *131*, 3464–3465; c) N. D. Shapiro, F. D. Toste, *J. Am. Chem. Soc.* **2008**, *130*, 9244-9245; d) B. Alcaide, P. Almendros, M. T. Quirós, I. F. Beilstein, *J. Org. Chem*. **2013**, *9*, 818–826; e) M. C. P. Yeh, H. F. Pai, Z. J. Lin, B. R. Lee, *Tetrahedron* **2009**, *65*, 4789-4794; f) P. C. Young, M. S. Hadfield, L. Arrowsmith, K. M. Macleod, R. J. Mudd, J. A. Jordan-Hore, A. L. Lee, *Org. Lett.* **2012**, *14*, 898–901; g) E. Jimenez-Nunez, M. Raducan, T. Lauterbach, K. Molawi, C. R. Solorio, A. M. Echavarren, *Angew. Chem. Int. Ed.* **2009**, *48*, 6152-6155; h) J. T. Bauer, M. S. Hadfield, A. L. Lee, *Chem. Commun.* **2008**, *44*, 6405−6407; i) M. S. Hadfield, J. T. Bauer, P. E. Glen, A. L. Lee, *Org. Biomol. Chem.* **2010**, *8*, 4090−4095; j) R. J. Mudd, P. C. Young, J. A. Jordan-Hore, G. M. Rosair, A. L. Lee, *J. Org. Chem.* **2012**, *77*, 7633−7639; k) T. Watanabe, S. Oishi, N. Fujii, H. Ohno, *Org. Let.* **2007**, *9*, 4821-4824; l) X. Cheng, L. Zhu, M. Lin, J. Chen, X. Huang, *Chem. Commun.* **2017**, *53*, 3745−3748; m) C. Li, Y. Zeng, H. Zhang, J. Feng, Y. Zhang, J. Wang, *Angew. Chem., Int. Ed*. **2010**, *49*, 6413−6417; n) X. Meng, M. Guo, J. Zhu, H. Zhu, X. Sun, L. Tian, Z. Cao, *Eur. J. Org. Chem.* **2019**, 2019, 1952−1956; o) D. Li, W. Zang, M. J. Bird, C. J. T. Hyland, M. Shi, *Chem. Rev*. **2021**, *121*, 8685−8755; p) C. C. Chintawar, A. K. Yadav, A. Kumar, S. P. Sancheti, N. T. Patil, *Chem. Rev.* **2021**, *121*, 8478−8558.

[12] J. F. Hartwig, *Organotransition Metal Chemistry, from Bonding to Catalysis*; University Science Books: New York, 2010.

[13] F. F. Mulks, P. W. Antoni, F. Rominger, A. S. K. Hashmi, *Adv. Synth. Catal.* **2018**, *360*, 1810-1821.

[14] N. Kim, R. A. Widenhoefer, *Chem. Sci.* **2019**, *10*, 6149-6156.

[15] S. Dupuy, A. M. Z. Slawin, S. P. Nolan, *Chem. Eur. J.* **2012**, *18*, 14923-14928.

[16] L. O'Brien, S. P. Argent, K. Ermanis, H. W. Lam, *Angew. Chem. Int. Ed.* **2022**, *61*, e202202305.

[17] For examples of gold (III) allyl complexes: a) S. Komiya, S. Ozaki, *Chem. Lett.* **1988**, *8*, 1431–1432; b) J. Rodriguez, G. Szallki, E. D. S. Carrizo, N. Saffon-Merceron, K. Miqueu, D. Bourissou, *Angew. Chem. Int. Ed*. **2020**, *59*, 1511 –1515; c) M. S. M. Holmsen, A. Nova, S. Øien-Ødegaard, R. H. Heyn, M. Tilset, *Angew. Chem. Int. Ed.* **2020**, *59*, 1516 –1520; d) T. Sone, S. Ozaki, N. C. Kasuga, A. Fakuoka, S. Komiya, *BCSJ* **1995**, *68*, 1523-1533; e) J. Rodriguez, M. S. M. Holmsen, Y. García-Rodeja, E. D. S. Carrizo, P. Lavedan, S. Mallet-Ladeira, K. Miqueu, D. Bourissou, *J. Am. Chem. Soc*. **2021**, *143*, 11568−11581.

[18] R. B. Ahmadi, P. Ghanbari, N. A. Rajabi, A. S. K. Hashmi, B. F. Yates, A. Ariafard, *Organometallics* **2015**, *34*, 3186−3195.

[19] L. O'Brien, S. P. Argent, K. Ermanis, H. W. Lam, *Angew. Chem. Int. Ed.* **2022**, *61*, e202202305.

[20] a) V. Gobe, M. Dousset, P. Retailleau, V. Gandon, X. Guincharda, *Adv. Synth. Catal.* **2016**, *358*, 3960 – 3965; b) V. Gobe, M. Dousset, P. Retailleau, V. Gandon, X. Guinchard, *J. Org. Chem.* **2018**, *83*, 898−912.

[21] A. S. K. Hashmi, A. M. Schuster, S. Litters, F. Rominger, M. Pernpointner, *Chem. Eur. J.* **2011**, *17*, 5661 – 5667.

[22] a) Y. T. Struchkov, Y. L. Slovokhotov, D. N. Kravtsov, T. V. Baukova, E. G. Perevalova, K. J. Grandberg, *J. Organomet. Chem.* **1988**, *338*, 269-280; b) T. V. Baukova, Y. L. Slovokhotov, Y. T. Struchkov, *J. Organomet. Chem.* **1981**, *220,* 125-137; c) E. G. Perevalova, K. J. Grandberg, V.P. Dyadchenko, T. V. Baukova, *J. Organomet. Chem.* **1981**, *217*, 403-413; d) M. Halim, R. D. Kennedy, M. Suzuki, S. I. Khan, P. L. Diaconescu, Y. Rubin, *J. Am. Chem. Soc.* **2011**, *133*, 6841–6851; e) H. Werner, H. Otto, T. Ngo-Khac, C. Burschka, *J. Organomet. Chem.* **1984**, *262*, 123-136; f) H. Schumann, F. H. Gorlitz, A. Dietrich, *Chem. Ber.* **1989**, *122*, 1423-1426; g) M. I. Bruce, J. K. Walton, B. W. Skelton, A. H. White, *J. Chem. Soc., Dalton Trans.* **1983**, 809-814; h) C. H. Campbell, M. L. H. Green, *J. Chem. Soc. A.* **1971**, 3282-3285.

[23] E. G. Perevalova, K. I. Grandberg, V. P. Dyadchenko, T. V. Baukova, *J. Organomet. Chem.* **1981**, *217*, 403-413.

[24] M. Stradiotto, D. W. Hughes, A. D. Bain, M. A. Brook, M. J. McGlinchey, *Organometallics* **1997**, *16*, 5563-5568.

[25] C. P. Casey, J. M. O'Connor, *Organometallics* **1985**, *4*, 384-388.

[26] T. Saegusa, Y. Ito, S. Tomita, *J. Am. Chem. Soc*. **1971**, *93*, 5656-5661.

[27] a) M. Stradiotto, M. J. McGlinchey, *Coord. Chem. Rev.* **2001**, *219–221*, 311–378; b) W. Kitching, B. F. Hegarty, *J. Organomet. Chem.* **1969**, *16*, 39-44; c) W. Kitching, B. F. Hegarty, D. Doddrell, *J. Organomet. Chem.* **1970**, *21*, 29-36: d) F. A. Cotton, D. L. Hunter, J. D. Jamerson, *Inorg. Chim. Acta* **1975**, *15*, 245-247; e) S. Bellomo, A. Ceccon, A. Gambaro, S. Santi, *J. Organomet. Chem.* **1993**, *453*, C4-C6; f) P. Cecchetto, A. Ceccon, A. Gambaro, S. Santi, P. Ganis, R. Gobetto, G. Valle, A. Venzo, *Organometallics* **1998**, *17*, 752-762; g) F. A. Cotton, A. Musco, G. Yagupsky, *J. Am. Chem. Soc.* **1967**, *89*, 6136-6139.

[28] a) G. S. Bates, S. Ramaswamy. *Can. J. Chem.* **1981**, *59*, 3120-3122; b) C. W. Spangler, Chem. Rev. **1976**, *76*, 187-217.

[29] T. J. Brown, M. G. Dickens; R. A. Widenhoefer, *Chem. Commun.* **2009**, 6451–6453.

[30] R. E. M. Brooner, R. A. Widenhoefer, *Angew. Chem.* **2013**, *125*, 11930-11941; *Angew. Chem. Int. Ed.* **2013**, *52*, 11714-11724.

[31] K. B. Wiberg, *Tetrahedron* **1968**, *24*, 1083–1096.

[32] A. Antušek, M. Blaško, M. Urban, P. Noga, D. Kisić, M. Nenadović, D. Lončarević and Z. Rakočevi, *Phys. Chem*. *Chem. Phys.* **2017**, *19*, 28897–28906.

[33] G. E. Jackson, J. R. Moss, L. G. Scott, *S. Afr. J. Chem.* **1983**, *36*, 69-72.

[34] a) G. Raper, W. S. McDonald, *Chem. Comm*. **1970**, 655; b) W. S. McDonald, B. E. Mann, G. Raper, B. L. Shaw, G. Shaw, *Chem. Comm*. **1969**, 1254; c) B. E. Mann, B. L. Shaw, G. Shaw, *J. Chem. Soc. A*. **1971**, 3536-3544; d) R. P. Hughes, J. Powell, *J. Organomet. Chem.* **1973**, *55*, C45-C48; e) B. P. Gracey, B. E. Mann, C. M. Spencer, *J. Organomet. Chem.* **1985**, *291*, 375-378.

[35] a) S. Hüffer, M. Wieser, K. Polborn, W. Beck, *J. Organomet. Chem.* **1994**, *481*, 45-55; b) H. J. Müller, U. Nagel, W. Beck, *Organometallics* **1987**, *6*, 193-194.

[36] S. Lotz, P. H. Van Rooyen, R. Meyer, *Adv. Organomet. Chem*. **1995**, *37*, 219-320.

[37] a) H. Werner, *Adv. Organomet. Chem*. **1981**, *19*, 155–182; b) N. Hazari, D. P. Hruszkewycz, *Chem. Soc. Rev*. **2016**, *45*, 2871-2899.

[38] a) R. Beck, S. A. Johnson, *Organometallics* **2013**, *32*, 2944-2951; b) J. Wu, A. Nova, D. Balcells, G. W. Brudvig, W. Dai, L. M. Guard, N. Hazari, P. H. Lin, R. Pokhrel, M. K. Takase, *Chem. Eur. J.* **2014**, *20*, 5327 – 5337.

[39] a) M. J. Chalkley, L. M. Guard, N. Hazari, P. Hofmann, D. P. Hruszkewycz, T. J. Schmeier, M. K Takase, *Organometallics* **2013**, *32*, 4223−4238; b) T. Tanase, T. Nomura, Y. Yamamoto, K. J. Kobayashi, *J. Organomet. Chem.* **1991**, 410, C25-C28; c) T. Tanase, T. Nomura, T. Fukushima, Y. Yamamoto, K. Kobayashi, *Inorg. Chem.* **1993**, *32*, 4578-4584.

[40] a) H. Kurosawa, K. Hirako, S. Natsume, S. Ogoshi, N. Kanehisa, Y. Kai, S. Sakaki, K. Takeuchi, *Organometallics* **1996**, *15*, 2089-2097; b) C. E. Housecroft, B. F. G. Johnson, J. Lewis, J. A. Lunnis, S. M. Owen, P. R. Raithby, *J. Organomet. Chem.* **1991**, *409*, 271-284; c) M. H. Chisholm, M. J. Hampden-Smith, J. C. Huffman, K. G. Moodley, *J. Am. Chem. Soc.* **1988**, *110*, 4070-4071; d) L. Zhu, N. M. Kostic, *Organometallics* **1988**, *7*, 665-669; e) S. Sakaki, K. Takeuchi, M. Sugimoto, H. Kurosawa, *Organometallics* **1997**, *16*, 2995-3003; f) S. Mecheri, B. Zouchoune, S. M. Zendaoui, *Theor. Chem. Acc.* **2020**, *139*, 12.

[41] R. G. Carden, N. Lam, R. A. Widenhoefer, *Chem. Eur. J.* **2017**, *23*, 17992–18001.

[42] Gaussian 16, Revision A.03, M. J. Frisch, G. W. Trucks, H. B. Schlegel, G. E. Scuseria, M. A. Robb, J. R. Cheeseman, G. Scalmani, V. Barone, G. A. Petersson, H. Nakatsuji, X. Li, M. Caricato, A. V. Marenich, J. Bloino, B. G. Janesko, R. Gomperts, B. Mennucci, H. P. Hratchian, J. V. Ortiz, A. F. Izmaylov, J. L. Sonnenberg, D. Williams-Young, F. Ding, F. Lipparini, F. Egidi, J. Goings, B. Peng, A. Petrone, T. Henderson, D. Ranasinghe, V. G. Zakrzewski, J. Gao, N. Rega, G. Zheng, W. Liang, M. Hada, M. Ehara, K. Toyota, R. Fukuda, J. Hasegawa, M. Ishida, T. Nakajima, Y. Honda, O. Kitao, H. Nakai, T. Vreven, K. Throssell, J. A. Montgomery, Jr., J. E. Peralta, F. Ogliaro, M. J. Bearpark, J. J. Heyd, E. N. Brothers, K. N. Kudin, V. N. Staroverov, T. A. Keith, R. Kobayashi, J. Normand, K. Raghavachari, A. P. Rendell, J. C. Burant, S. S. Iyengar, J.

Tomasi, M. Cossi, J. M. Millam, M. Klene, C. Adamo, R. Cammi, J. W. Ochterski, R. L. Martin, K. Morokuma, O. Farkas, J. B. Foresman, and D. J. Fox, Gaussian, Inc., Wallingford CT, **2016**.

[43] a) A. D. Becke, *J. Chem. Phys.* **1993**, *98*, 5648-5652; b) C. Lee, W. Yang, R. G. Parr, *Phys. Rev. B* **1988**, *37*, 785–789.

[44] W. J. Hehre, L. Radom, P. V. R. Schleyer, J. A. Pople. Ab Initio Molecular Orbital Theory; Wiley: New York, **1986**.

[45] a) D. Figgen, G. Rauhut, M. Dolg, H. Stoll, *Chem. Phys.* **2005**, *311*, 227–244; b) K. A. Peterson, C. Puzzarini, *Theor. Chem. Acc.* **2005**, *114*, 283–296.

[46] J. Tao, J. P. Perdew, V. N. Staroverov, G. E. Scuseria, *Phys. Rev. Lett.* **2003**, *91*, 146401.

[47] a) T. H. Dunning, Jr. *J. Chem. Phys.* **1989**, *90*, 1007–1023; b) D. E. Woon, T. H. Dunning, Jr. *J. Chem. Phys*. **1993**, *98*, 1358–1371; c) A. K. Wilson, D. E. Woon, K. A. Peterson, T. H. Dunning, Jr. *J. Chem. Phys.* **1999**, *110*, 7667–7676.

[48] A. V. Marenich, C. J. Cramer, D. G. Truhlar. *J. Phys. Chem. B* **2009**, *113*, 6378–6396.

Entry for the Table of Contents

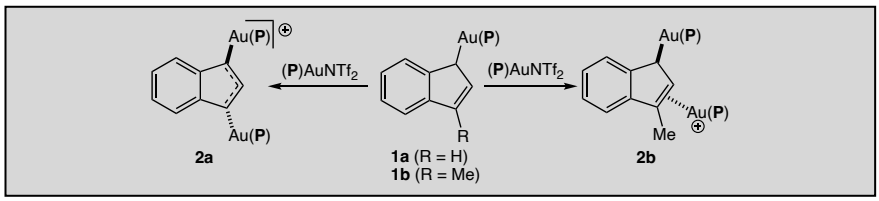

Reaction of the gold η^1-indenyl complexes (**P**)Au(η^1-inden-1-yl) (**1a**) and (**P**)Au(η^1-3-methylinden-1-yl) (**1b**) [**P** = P(*t*-Bu)$_2$*o*-biphenyl] with (**P**)AuNTf$_2$ forms the corresponding cationic bis(gold) indenyl complexes *trans*-[(**P**)Au]$_2$(η^1,η^1-inden-1,3-yl) (**2a**) and *trans*-[(**P**)Au]$_2$(η^1,η^2-3-methylinden-1-yl) (**2b**), respectively. The binding affinity of complexes **1a** and **1b** toward exogenous (**P**)Au$^+$ significantly exceeds that of free indene and 3-methylindene, respectively. Protodeauration of **2a** is significantly slower than is protodeauration of **1a**.

Institute and/or researcher Twitter usernames: ((optional))